Batch Clipping and Adaptive Layerwise Clipping for Differential Private Stochastic Gradient Descent

Toan N. Nguyen[1*], **Phuong Ha Nguyen**[2*], **Lam M. Nguyen**[3],**Marten van Dijk**[4,5,6]

[1] Department of Computer Science and Engineering, University of Connecticut, CT, USA
[2] eBay, CA, USA
[3] IBM Research, Thomas J. Watson Research Center, Yorktown Heights, NY, USA
[4] CWI Amsterdam, The Netherlands
[5] Department of Computer Science, Vrije Universiteit Amsterdam, The Netherlands
[6] Department of Electrical and Computer Engineering, University of Connecticut, CT, USA

`toan.nguyen@uconn.edu, phuongha.ntu@gmail.com,`
`LamNguyen.MLTD@ibm.com, marten.van.dijk@cwi.nl`

ABSTRACT

Each round in Differential Private Stochastic Gradient Descent (DPSGD) transmits a sum of clipped gradients obfuscated with Gaussian noise to a central server which uses this to update a global model which often represents a deep neural network. Since the clipped gradients are computed separately, which we call Individual Clipping (IC), deep neural networks like resnet-18 cannot use Batch Normalization Layers (BNL) which is a crucial component in deep neural networks for achieving a high accuracy. To utilize BNL, we introduce Batch Clipping (BC) where, instead of clipping single gradients as in the orginal DPSGD, we average and clip batches of gradients. Moreover, the model entries of different layers have different sensitivities to the added Gaussian noise. Therefore, Adaptive Layerwise Clipping methods (ALC), where each layer has its own adaptively finetuned clipping constant, have been introduced and studied, but so far without rigorous DP proofs. In this paper, we propose *a new ALC and provide rigorous DP proofs for both BC and ALC*. Experiments show that our modified DPSGD with BC and ALC for CIFAR-10 with resnet-18 converges while DPSGD with IC and ALC does not.

1 Introduction

Differential Private Stochastic Gradient Descent (DPSGD) [1] combines Stochastic Gradient Decent (SGD) [19] and Differential Privacy (DP)[8] to train deep neural networks privately. It has been widely studied since its introduction.

In each round of DPSGD a mini-batch of m samples $\xi_{i_1}, \ldots, \xi_{i_m}$ from a larger data set $d = \{\xi_i\}_{i=1}^{N}$ of N samples is randomly subsampled:

$$\{i_1, \ldots, i_m\} \leftarrow \texttt{Sample}_m(N). \tag{1}$$

The global model w is updated by first computing gradients $\nabla_w f(w; \xi_{i_j})$ for each sample ξ_{i_j} given loss function f. Each gradient is clipped by using a clipping operation $[x]_C = x/\max\{1, \|x\|/C\}$ where C denotes a fixed clipping constant. The clipped gradients are aggregated in a sum after which a noise vector n drawn from a Gaussian distribution* $\mathcal{N}(0, (2C\sigma\mathbf{I})^2)$ is added. The resulting "noised and clipped" update U is transmitted to a central server where it is

---

* these authors contributed equally.

*$\mathbf{I}$ is the identity correlation matrix of the multivariate Gaussian distribution. The factor 2 is due to sampling exactly m data points every round; by using a Poisson process to probabilistically sample $\xi \in d$ such that in expectation the mini-batch has size m removes the factor 2 and leads to better DP. This is implemented in [18]. In order to simplify our exposition we work with deterministic sampling and keep the factor 2.

averaged over the size m of the used mini-batch and multiplied by a step-size μ before subtracting it from the global model:

$$U \quad := \quad n + \sum_{j=1}^{m} [\nabla_w f(w; \xi_{i_j})]_C \quad \text{and} \quad w := w - \frac{\eta}{m} U. \tag{2}$$

In DPSGD, σ translates to a DP guarantee and is chosen carefully by the designer to balance DP and the accuracy of the final global model.

The global model is represented by a weight vector w which can be written as a concatenation $(w_1 | \ldots | w_L)$ where w_h corresponds to the h-th layer in the neural network which is being trained. DPSGD uses a fixed clipping constant C for clipping gradients

$$\nabla_w f(w; \xi_{i_j}) = (\nabla_{w_1} f(w; \xi_{i_j}) | \ldots | \nabla_{w_L} f(w; \xi_{i_j})).$$

In expectation the norms $\|\nabla_{w_h} f(w; \xi_{i_j})\|$ of different layers h in a deep neural network model vary layer by layer. This makes different layers have different sensitivity to the added Gaussian noise. For this reason, [20, 21, 22] proposed† Adaptive Layerwise Clipping (ALC) which tunes the added Gaussian noise with respect to the (sensitivity of the) layer. Each layer of the model has its own customized clipping constant based on estimating the expectation of the gradient norms of each layer by sampling a given small public dataset $\mathcal{D}_{pub}$. We notice that [20, 21, 22] have not provided rigorous DP proofs for ALC. In this paper we prove DP guarantees for ALC and we enhance the ALC method of [22] for improved test accuracy.

Besides the enhanced ACL, we introduce Batch Clipping (BC) where (2) is replaced by

$$U \quad := \quad n + \left[\frac{1}{m} \sum_{j=1}^{m} \nabla_w f(w; \xi_{i_j}) \right]_C \quad \text{and} \quad w := w - \eta U. \tag{3}$$

BC allows us to first compute an average of a batch of gradients before clipping, as opposed to (2) which averages a sum of clipped individual gradients; for this reason we call (2) the Individual Clipping (IC) approach. BC gives us the ability to properly train Batch Normalization Layers (BNL) [13] in a neural network; in very deep neural networks the use of BNLs is crucial for achieving high accuracy. The BC and ALC techniques are complimentary and can be implemented in parallel, also BC and ALC do not require any changes to be made in deep neural networks, i.e., BC and ALC apply directly without modifications to the neural network that we wish to train. This makes our training framework with BC and ALC flexible. BC allows us to use resnet-18[11] (which uses BNLs) in our experiments and have a DP guarantee. DPSGD without BC cannot properly train BNLs, therefore, DPSGD with IC (even with ALC) for resnet-18 does not converge and leads to poor accuracy, while DPSGD with BC and the enhanced ALC does converge. In the context of DPSGD we are the first to introduce BC together with proving its DP guarantee; no prior related work on DPSGD with BC exists.

Our main contribution are:

- We propose an enhanced Adaptive Layerwise Clipping method based on [22]. Our experiments show that DPSGD with our enhanced ALC converges faster to a higher accuracy.

- We prove and characterize the DP guarantee for ALC by using the f-DP framework [5]. We explain how layerwise clipping degrades DP and we show how to set the noise parameters of DPSGD without ALC and DPSGD with ALC so that they have the same DP guarantee and their test accuracy can be fairly compared.

- We introduce and propose to use Batch Clipping during training. We also define General Batch Clipping (GBC) of which BC and IC are special cases and notice that GBC is compatible with *any first order optimizers* in mini-batch mode. BC allows us to implement Batch Normalization Layers which are crucial for attaining high accuracy for deep neural networks (BNLs cannot be trained properly by the original DPSGD which uses Individual Clipping).

- For proving differential privacy guarantees it is commonly understood that the privacy argument does not depend on how the gradients in the clipped values in (2) are computed; the to-be-clipped values may as well be computed as in (3). This shows that (the original) DPSGD with IC given by (2) and (the new) DPSGD with BC given by (3) offer the exact same DP guarantee (also if both implement ALC).

- Our experiments show that DPSGD modified by using our enhanced ACL and using BC allows us to train the deep neural network resnet-18 [11] (which uses BNL) on CIFAR10 [14] while DPSGD with ALC and IC does not converge. This shows that BC outperforms IC in practice.

---

†For completeness, per-layer clipping was originally introduced in DP-FEDAVG [16] where a clipping budget is *evenly* (not customized) distributed among all layers and a DP guarantee is proven based on the moment accountant from [1].

Our main conclusion is that ACL and BC are two techniques that provide a better balance between DP and accuracy. However, our experiments are for small σ which corresponds to weak differential privacy. We still need additional techniques beyond ALC and BC for training a deep neural network like resnet-18 with CIFAR10 in order to achieve a practical balance between test accuracy and DP guarantee.

Outline: We first provide the necessary background on f-DP in Section 2. Section 3 introduces BC (and GBC), layerwise clipping and our ACL, and proves DP guarantees in the f-DP framework. Experiments are in Section 4. Section 5 concludes our paper.

2 Background on f-DP

DP literature first introduced ϵ-DP [9], later relaxed to (ϵ, δ)-DP [10]. In order to have a better dependency on group privacy and to improve adaptive composibility, the notion of Concentrated Differential Privacy (CDP) [7] was introduced. CDP was re-interpreted and relaxed by using Renyi entropy in [2] and its authors followed up with the notion of zero-CDP (zCDP) in [3]. This notion admits simple interpretable DP guarantees for adaptive composition and group privacy. After the introduction of ρ-zCDP, Renyi DP (RDP) was introduced by [17]. Combining the ideas that give rise to the zCDP and RDP definitions leads naturally to the definition of (ρ, ω)-tCDP [4] which relaxes zCDP. All of these various DP measures have been superseded by f-DP [6]since (1) f-DP can be transformed/translated into divergence based DP guarantees (but generally not the other way around) and can be translated into (ϵ, δ)-DP, and since (2) f-DP analyses the underlying core hypothesis testing problem directly and derives a *tight* (or exact) DP guarantee (for the adversarial model considered in the proofs of DP guarantees in literature). The f-DP framework is tight and contains all the information needed to derive other known DP metrics. Below we summarize f-DP and show how to use f-DP to prove and formulate the DP guarantee of our modified DPSGD algorithm.

We call data sets $d = \{\xi_i\}_{i=1}^N$ and $d' = \{\xi_i'\}_{i=1}^N$ neighboring if they differ in one element; without loss of generality $\xi_i = \xi_i'$ for $1 \le i \le N-1$ and $\xi_N \ne \xi_N'$ coined the *differentiating sample*. In DP a mechanism $\mathcal{M}$ is a process that takes either data set d or data set d' as input and outputs a sequence of observables which the adversary uses to distinguish which of d or d' has been used. DPSGD is a mechanism which outputs a sequence of updates U corresponding to each round, see (2). Below, we adopt the notion and explanation provided in [5] for our short introduction of f-DP. We refer the reader to [5] for a full description.

Hypothesis Testing: From the attacker's perspective, it is natural to formulate the problem of distinguishing two neighboring data sets d and d' based on the output of a DP mechanism $\mathcal{M}$ as a hypothesis testing problem:

$$\text{versus} \quad \begin{array}{l} H_0 : \text{ the underlying data set is } d \\ H_1 : \text{ the underlying data set is } d'. \end{array}$$

We define the Type I and Type II errors by

$$\alpha_\phi = \mathbb{E}_{o \sim \mathcal{M}(d)}[\phi(o)] \text{ and } \beta_\phi = 1 - \mathbb{E}_{o \sim \mathcal{M}(d')}[\phi(o)],$$

where ϕ in $[0, 1]$ denotes the rejection rule which takes the output of the DP mechanism as input. We flip a coin and reject the null hypothesis with probability ϕ. The optimal trade-off between Type I and Type II errors is given by the trade-off function

$$T(\mathcal{M}(d), \mathcal{M}(d'))(\alpha) = \inf_\phi \{\beta_\phi \ : \ \alpha_\phi \le \alpha\},$$

for $\alpha \in [0, 1]$, where the infimum is taken over all measurable rejection rules ϕ. If the two hypothesis are fully indistinguishable, then this leads to the trade-off function $1 - \alpha$. We say a function $f \in [0, 1] \to [0, 1]$ is a trade-off function if and only if it is convex, continuous, non-increasing, at least 0, and $f(x) \le 1 - x$ for $x \in [0, 1]$. We define a mechanism $\mathcal{M}$ to be f-DP if f is a trade-off function and for all neighboring d and d',

$$T(\mathcal{M}(d), \mathcal{M}(d')) \ge f.$$

Gaussian DP: Gaussian DP is defined as a special case of f-DP where f is defined as a trade-off function

$$G_\mu(\alpha) = T(\mathcal{N}(0, 1), \mathcal{N}(\mu, 1))(\alpha) = \Phi(\Phi^{-1}(1 - \alpha) - \mu),$$

for some $\mu \ge 0$, where Φ is the standard normal cumulative distribution of $\mathcal{N}(0, 1)$. Suppose that a mechanism $\mathcal{M}(d)$ computes some function $u(d) \in \mathbb{R}^n$ and adds Gaussian noise $\mathcal{N}(0, (c\sigma)^2 \mathbf{I})$, that is, the mechanism outputs $o \sim u(d) + \mathcal{N}(0, (C\sigma)^2 \mathbf{I})$. Suppose that c denotes the sensitivity of function $u(\cdot)$, that is,

$$\|u(d) - u(d')\| \le c$$

3

for neighboring d and d'; the mechanism corresponding to one round update in DPSGD, where $\texttt{Sample}_m(N)$ selects (as one of the m randomly selected indices) the index N of the differentiating sample, has *sensitivity* $c = 2C$. After projecting the observed o onto the line that connects $u(d)$ and $u(d')$ and after normalizing by dividing by c, we have that differentiating whether o corresponds to d or d' is in the best case for the adversary (i.e., $\|u(d) - u(d')\| = c$) equivalent to differentiating whether a received output is from $\mathcal{N}(0, \sigma^2)$ or from $\mathcal{N}(1, \sigma^2)$. Or, equivalently, from $\mathcal{N}(0, 1)$ or from $\mathcal{N}(1/\sigma, 1)$. This is how the Gaussian trade-off function $G_{\sigma^{-1}}$ comes into the picture.

Subsampling: Besides implementing Gaussian noise which bootstraps DP, DPSGD also uses $\texttt{Sample}_m$ for subsampling which amplifies DP. [6] defines a subsampling operator $C_{m/N}$ and shows that if a mechanism $\mathcal{M}$ on data sets of size N is f-DP, then the subsampled mechanism $\mathcal{M} \circ \texttt{Sample}_m$ is $C_{m/N}(f)$-DP. We have that the mechanism corresponding to one round in DPSGD is $C_{m/N}(G_{1/\sigma})$-DP (and this is a tight analysis).

Composition: If DPSGD implements T rounds, then the privacy leakage across rounds composes. [6] defines a commutative tensor product $\otimes$ for trade-off functions and shows this can be used to characterize adaptive composibility: Let $\mathcal{M}_i$ be the mechanism corresponding to the i-th round with $y_i \leftarrow \mathcal{M}_i(\texttt{aux}, d)$ where $\texttt{aux} = (y_1, \ldots, y_{i-1})$ (this captures adaptivity). If $\mathcal{M}_i(\texttt{aux}, .)$ is f_i-DP for all $\texttt{aux}$, then the composed mechanism $\mathcal{M}$, which applies $\mathcal{M}_i$ in sequential order from $i = 1$ to $i = T$, is $(f_1 \otimes \ldots \otimes f_T)$-DP. This leads to a tight analysis of DPSGD. We have that DPSGD as introduced in [1] is

$$C_{m/N}(G_{1/\sigma})^{\otimes T}\text{-DP}.$$

Notice that if DPSGD computes a total of E epochs of gradients, i.e., EN gradient computations in total, then $T = (N/m) \cdot E$ (since each round computes m gradients). We have

$$C_{m/N}(G_{1/\sigma})^{\otimes (N/m) \cdot E}\text{-DP}. \tag{4}$$

3 Application f-DP toward a Modified DPSGD

We discuss two main DPSGD modifications. The first is coined Batch Clipping (BC) and the second Layerwise Clipping (LC) leading to Adaptive LC (ACL).

3.1 Batch Clipping

The presented f-DP analysis is more general in that it holds for (2) where U is not just computed as a noised sum of clipped *gradients* but computed as

$$U := n + \sum_{j=1}^{m} [g(w; \xi_{i_j})]_C \tag{5}$$

for some other fixed function g.

Suppose that we partition data set d of size N into N/s mini-sets of size s each. We use this to define a new data set d_s which has as elements the N/s mini-sets, which we denote as S_i, $1 \leq i \leq N/s$. Data set d_s has size N/s and its samples are mini-sets S_i of size s. Each S_i contains s data points ξ_j from d. We apply DPSGD to this new data set d_s for the general (5) where we replace m by k. This yields

$$U := n + \sum_{j=1}^{k} [g(w; S_{i_j})]_C. \tag{6}$$

We call this General Batch Clipping (GBC) since we clip vectors $g(w; S_{i_j})$ which are computed based on a batch (mini-set) $S_{i_j} \subseteq d$ of data points from d. Notice that in GBC, g can implement any moment based SGD type algorithm that iteratively scans the data points in S_{i_j}.

Applying the f-DP analysis for DPSGD for a data set d_s of size N/s with $\texttt{Sample}_k$, see (6), yields $C_{k/(N/s)}(G_{1/\sigma})^{\otimes T}$-DP, see Section 2. By setting $m = sk$, we conclude $C_{m/N}(G_{1/\sigma})^{\otimes T}$-DP. Notice that if the modified DPSGD with GBC computes a total of E epochs of gradients, then again $T = (N/m) \cdot E$ since each round still computes $m = sk$ gradients. For GBC with $m = sk$ we conclude the exact same DP guarantee as the one for (4).

In our experiments we use the special case

$$g(w; S_{i_j}) = \frac{1}{s} \sum_{\xi \in S_{i_1}} \nabla_w f(w; \xi) \tag{7}$$

4

with $k = 1$ and $s = m$ in GBC (with $m = sk$). We refer to this as (non-general) Batch Clipping (BC) (since we clip $g(w; S_{i_1})$ which computes and averages a batch of gradients), see (3). We call the original DPSGD formulation (2) Individual Clipping (IC) since single/individual gradients are clipped; for completeness, this is the case $s = 1$ with $k = m$ in GBC (with $m = sk$).

3.2 Layerwise Clipping

Layerwise Clipping (LC) [16, 20, 21, 22] splits vectors $g = g(w; S_{i,j})$ in parts $g = (g_1 | \ldots | g_L)$ (i.e., g is equal to the concatenation of parts g_1, ..., g_L) and clip each part g_h separately, i.e., we define

$$[g]_{(C_1, \ldots, C_L)} = ([g_1]_{C_1} | \ldots | [g_L]_{C_L}).$$

The different g_i correspond to the different layers in the neural network. We compute noise n in (6) as the concatenation

$$n = (n_1 | \ldots | n_L) \quad \text{with} \quad n_h \sim \mathcal{N}(0, (2C_h \sigma)\mathbf{I}),$$

where the different matrices $\mathbf{I}$ have sizes that correspond to the number of entries in the various g_h.

In order to understand how the DP guarantee is affected, we rewrite (6) as follows:

$$U := (U_1 | \ldots | U_L) \quad \text{where} \quad U_h = n_h + \sum_{j=1}^{k} [g_h(w; S_{i_j})]_{C_h}.$$

In other words, transmission of U is equal to transmitting U_h, $1 \leq h \leq L$. Each U_h can be considered as a round update where we use clipping constant C_h and noise $\mathcal{N}(0, (2C_h \sigma)\mathbf{I})$. The f-DP analysis shows that such a round is $G_{1/\sigma}$-DP (see the explanation of Gaussian DP with sensitivity $c = 2C_h$). We have L such sub-rounds that make up the whole transmission of U. By composition, we have that this gives $G_{1/\sigma}^{\otimes L}$-DP. [6] shows that[‡] $G_{1/\sigma}^{\otimes L} = G_{\sqrt{L}/\sigma}$.

We conclude that in the DP guarantee (4) we need to replace σ by $\sigma/\sqrt{L}$ for the modified DPSGD with BC/IC and LC. If we want to compare this in a fair way with the modified DPSGD with BC/IC and *no* LC (we keep the original gradient clipping approach), then we should use

$$\bar{\sigma} := \sigma/\sqrt{L}$$

as the privacy parameter σ in the modified DPSGD (as this will result in the same (4) with σ replaced by $\bar{\sigma} = \sigma/\sqrt{L}$).

Clearly, we want to be careful about the number of layers L we can handle since the privacy parameter σ is divided by $\sqrt{L}$. We notice that we can group layers together and split vectors $g = g(w; S_{i,j})$ into a smaller number of parts giving a smaller L which leads to a better DP guarantee.

3.3 Adaptive LC

The Adaptive LC (ALC) of [22] uses a public dataset $\mathcal{D}_{pub}$ to estimate expectations of the layer gradient norms $\|\nabla_{w_h} f(w; \xi)\|$. These estimates are used as the layerwise clipping constants C_h. For standard SGD without DP, [12] explains that even if model w converges, the gradient norms of different layers may not decrease throughout the training. We confirm this in Figure 1, which depicts layer gradient norms of resnet-18 trained without DP over 50 epochs. We observe that most layer gradient norms only slowly decrease from epoch to epoch. Therefore, most of the C_h in the ALC of [22] are only slightly adapted from epoch to epoch. This implies that, for such a layer h, the distribution $\mathcal{N}(0, (2C_h \sigma)^2 \mathbf{I})$ of the Gaussian noise added to each of the weight entries in layer h does not change much either. This setup does not allow the designer to optimize the clipping constants $C_1, \ldots, C_L$ to make convergence faster.

We enhance the adaptive clipping strategy of [22]: First, we determine a master clipping constant C for each round. We do not impose a restriction on how C is chosen, i.e., it can diminish from epoch to epoch or C can be the same constant for all rounds. In our experiments C is a constant throughout the whole training. Second, we use C to derive clipping values $(C_1, C_2, ..., C_L)$ for the corresponding round. This has the property that each C_h scales linearly with C.

Given a master clipping constant C at the beginning of each round, we use a *public* dataset $\mathcal{D}_{pub}$ to derive clipping constants $(C_1, C_2, ..., C_L)$. The reason for using a public dataset is that we do not need to worry about privacy leakage revealed by $(C_1, C_2, ..., C_L)$; DP analysis/proofs, where the adversary knows $(C_1, C_2, ..., C_L)$, may proceed as before. We estimate the expectation $e = (e_1, \ldots, e_L)$ of the layer gradient norms $(\|\nabla_{w_1} f(w; \xi)\|, \ldots, \|\nabla_{w_L} f(w; \xi)\|)$ over $\xi \in \mathcal{D}_{pub}$ for $w = (w_1 | \ldots | w_L)$. We compute the maximum gradient norm among all layers, i.e., $M = \max_{h=1}^{L} e_h$. Then, for each layer h we define $C_h = C \cdot e_h / M$. See Section 4.4, Figure 4 shows that our enhanced ALC allows DPSGD with BC to converge faster to a higher accuracy compared to DPSGD with BC and the original ALC of [22].

[‡]We can also vary the noise from layer to layer and use σ/p_h instead of σ. This leads to $G_{p_1/\sigma} \otimes \ldots \otimes G_{p_L/\sigma} = G_{\sqrt{\sum_{h=1}^{L} p_h^2}/\sigma}$.
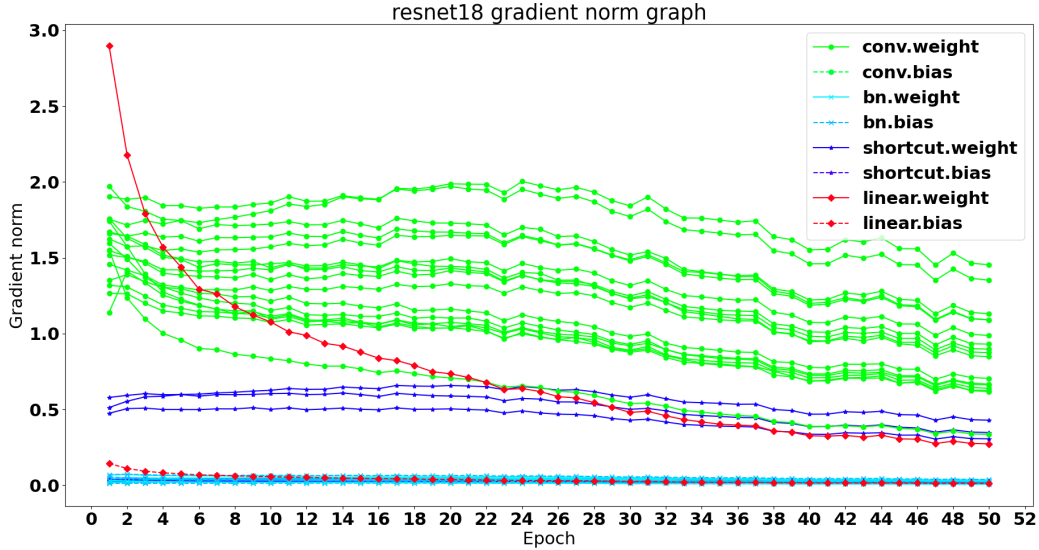
Figure 1: resnet-18 model layerwise gradient norms. We grouped the lines by the layer's type: "conv" is convolutional layer, "bn" is the batch normalization layer, "shortcut" is the shortcut connecting non-adjacent two layers, "linear" is the fully connected layer (in this case this layer corresponds to a softmax layer)

3.4 Sparsification

We notice that the public data set $\mathcal{D}_{pub}$ in adaptive clipping can also be used to find out whether certain weight entries in w have converged sufficiently. That is, we say a weight entry has converged if, over a large number of recent rounds, it hoovers around an average with standard deviation corresponding to the added DP noise. As soon as this is the case, we may fix the weight entry to this average in all future computations/rounds (since this is a form of post processing, no additional DP leakage occurs). This reduces the number of weight entries over which we need to compute gradients and each level gets less weight entries as soon as convergence sets in. This allows us to use even smaller clipping constants per layer (depending on the number of active weight entries in the layers). We leave this optimization as an open problem.

4 Experiments

4.1 Setup

Data preprocessing: We perform experiments on the CIFAR-10 dataset which consists of 50,000 training examples and 10,000 test examples, divided into 10 classes, with each example being a 32x32 image with three color channels (RGB)([14]). In our experiments, we perform data augmentation and data normalization independently. Specifically, for each training image, we crop a 32×32 region from it with padding of 4, apply a random horizontal flip to the image, and then normalize it with

$$(mean, std) = ((0.4914, 0.4822, 0.4465), (0.2023, 0.1994, 0.2010)).$$

Next, we divide the CIFAR-10 dataset $\mathcal{D}$ into two dataset $\mathcal{D}_{pub}$ and $\mathcal{D}_{train}$ where $|\mathcal{D}_{pub}| = \frac{1}{10}|\mathcal{D}|$ and $|\mathcal{D}_{train}| = \frac{9}{10}|\mathcal{D}|$.

As explained in Section 3.3, we estimate the expectation $(e_1, \ldots, e_L)$ of the layer gradient norms $(\|\nabla_{w_1} f(w; \xi)\|, \ldots, \|\nabla_{w_L} f(w; \xi)\|)$ over[§] $\xi \in \mathcal{D}_{pub}$, where $w = (w_1 | \ldots | w_L)$ is the current model. We compute the layerwise clipping constants $(C_1 = C \cdot e_1/M, \ldots, C_L = C \cdot e_L/M)$ with $M = \max_{h=1}^{L} e_h$ and master clipping constant C.

We sample the m-sized training data batches with replacement from $\mathcal{D}_{train}$ at the beginning of each epoch and feed them to the machine learning model to train the model.

[§]We notice that we may not need a large sized $\mathcal{D}_{pub}$ for a good estimate.

6

Diminishing Learning Rate and Fixed Master Clipping Constant: We fix the master clipping constant C throughout the training process and after each epoch we update the learning rate η as

$$\eta \quad := \quad \eta \cdot \eta_{decay},$$

where η_{decay} is a decaying factor. After each epoch, we re-compute the layerwise clipping constants $(C_1, C_2, \ldots, C_L)$ as explained above. In our experiments, we set $\eta_{decay} = 0.9$, $C = 0.095$ and $\sigma = 0.01875$.

Model Update: resnet-18 is updated by our modified DPSGD with BC and ALC, i.e., for a batch (mini-set) $\{\xi_{i_1}, \ldots, \xi_{i_m}\}$ we compute

$$U \quad := \quad n + \left[\frac{1}{m}\sum_{j=1}^{m}\nabla_w f(w; \xi_{i_j})\right]_{(C_1, \ldots, C_L)} \quad \text{and} \quad w := w - \eta U$$

with $n \sim \mathcal{N}(0, (2C_1\sigma)^2\mathbf{I}) \times \ldots \times \mathcal{N}(0, (2C_L\sigma)^2\mathbf{I})$.

4.2   Benchmark versus BC

We compare our DPSGD with BC and ALC versus mini-batch SGD without DP, i.e., without clipping and without adding Gaussian noise. In both cases, we train resnet-18 on the CIFAR-10 dataset.

For mini-batch SGD with diminishing learning rate without DP we experiment with mini-batch sizes $m = (64, 128, 256, 512, 1024)$ and initial learning rate $\eta = 0.025$. The best test accuracy at epochs 20 and 50 is realized by mini-batch size $m = 64$ and achieves 88.31% and 90.24% (see Figure 2). The results of our DPSGD with BC and ALC and diminishing learning rate, with fixed master clipping constant $C = 0.0095$, with standard deviation $\sigma = 0.01875$, and with $m = (64, 128, 256, 512, 1024)$ and initial learning rate $\eta = 0.025$ are presented in Figure 3. We achieve 60% and 67% at epochs 20 and 50 for $m = 64$.
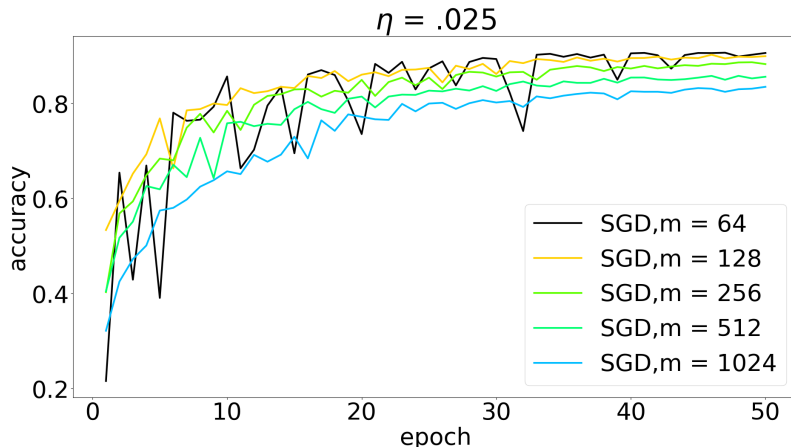

Figure 2: Test accuracies of mini-batch SGD without DP for different mini-batch sizes $m = (64, 128, 256, 512, 1024)$

4.3   IC versus BC

We compare our DPSGD with BC and ALC versus DPSGD with IC and the same ALC. The latter is the original DPSGD [1] combined with ALC. Based on the result from Section 4.2, we choose $m = 64$ which gives the best test accuracy for fixed master clipping constant $C = 0.0095$ and initial learning rate $\eta = 0.025$. We report the test accuracies after $E = 50$ epochs for $\sigma = 0.01875$ in Figure 4. We observe that BC converges while IC does not.

4.4   Zhang's ALC versus ours

As discussed in Section 3.3, the layerwise clipping constants $C_1, \ldots, C_L$ in [22] may not change from epoch to epoch because the layer gradient norms of resnet18 do not significantly change throughout the training process as depicted in Figure 1. We explained that this may hurt the convergence if $C_1, \ldots, C_L$ are not optimized. Based on this observation, our proposed enhanced ALC implements a master clipping constant C which allows us to optimize layer clipping
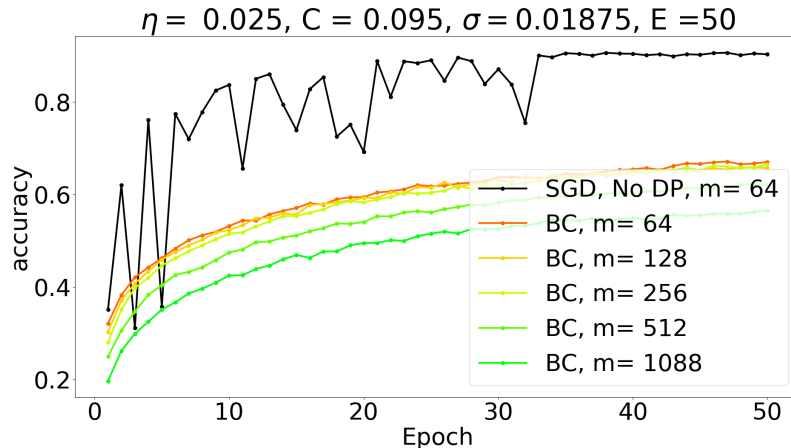
Figure 3: Test accuracies of DPSGD+BC+ALC vs mini-batch SGD without DP for different mini-batch sizes $m = (64, 128, 256, 512, 1024)$

constants $C_1, \ldots, C_L$. By tuning the initial/fixed master clipping constant C, DPSGD with BC and our enhanced ALC offers a better performance compared to DPSGD with BC and the ALC method of [22].

We run DPSGD with BC and the our enhanced ALC method with initial learning rate $\eta = 0.025$, fixed master clipping constant $C = 0.0095$, and $m = 64$ over 50 epochs for resnet-18 and CIFAR-10. We run DPSGD with BC and the ALC of [22] with the same learning rate $\eta = 0.025$ and $m = 64$ over 50 epochs for resnet-18 and CIFAR-10. The results are shown in Figure 4.
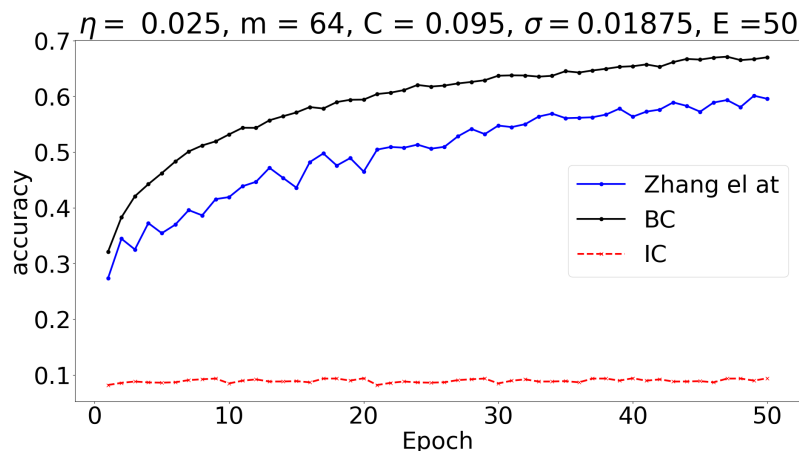

Figure 4: Comparison of the test accuracies between our enhanced ALC and the ALC method of [22], both with BC. Moreover, we run our enhanced ALC in IC mode so that we can also compare BC versus IC. ("Zhang et al." denotes DPSGD + BC + ALC of [22]; "BC" denotes DPSGD + BC + our enhanced ALC; "IC" denotes DPSGD + IC + our enhanced ALC)

4.5 Different noises

We study the relationship between the test accuracy and σ for DPSGD with BC and the enhanced ALC with $\eta = 0.025$, $m = 64$, and $C = 0.095$ over 10 epochs. The result is depicted in Figure 5 and shows that for convergence resnet-18 needs a relatively small σ and as a consequence can only achieve a weak DP guarantee. This shows that a proper balance between test accuracy and DP guarantee for very deep neural networks with complex datasets is still an open problem. Our BC and ALC techniques help towards achieving a practical balance, but more complimentary tricks and methods are still needed.
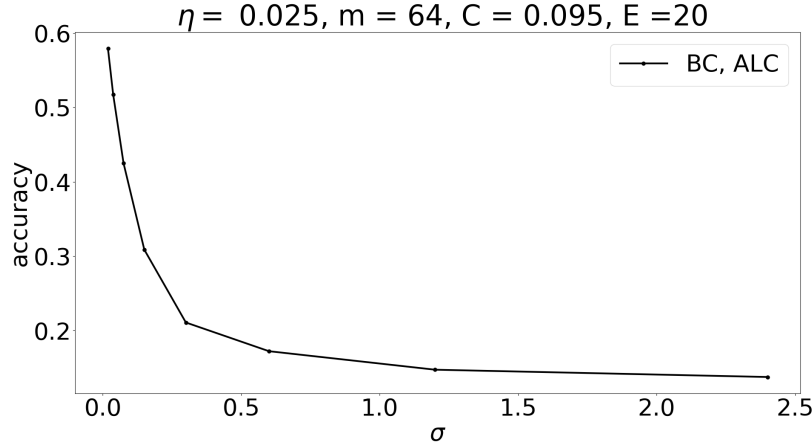
8

Figure 5: The test accuracy of the modified DPSGD with BC and enhanced ALC for different σ over 10 epochs.

5 Conclusion

We have proposed a new adaptive layerwise clipping method as well as a new batch clipping method for DPSGD. Our experiments show that DPSGD with BC and new ALC can achieve faster convergence and higher accuracy compared to DPSGD with IC. We have provided rigorous DP proofs for ALC and BC.

Our experiments are for small σ which leads to weak differential privacy. We still need additional techniques beyond (optimizing) ALC and BC for training a deep neural network like resnet-18 with CIFAR10 in order to achieve a practical balance between test accuracy and DP guarantee.

References

[1] Martin Abadi, Andy Chu, Ian Goodfellow, H Brendan McMahan, Ilya Mironov, Kunal Talwar, and Li Zhang. Deep learning with differential privacy. In *Proceedings of the 2016 ACM SIGSAC Conference on Computer and Communications Security*, pages 308–318. ACM, 2016.

[2] Mark Bun and Thomas Steinke. Concentrated differential privacy: Simplifications, extensions, and lower bounds. *arXiv*, 2016.

[3] Mark Bun and Thomas Steinke. Concentrated differential privacy: Simplifications, extensions, and lower bounds. In Martin Hirt and Adam D. Smith, editors, *TCC*, volume 9985, pages 635–658, 2016.

[4] Mark Bun, Cynthia Dwork, Guy N. Rothblum, and Thomas Steinke. Composable and versatile privacy via truncated CDP. In Ilias Diakonikolas, David Kempe, and Monika Henzinger, editors, *STOC*. ACM, 2018.

[5] Jinshuo Dong, Aaron Roth, and Weijie J. Su. Gaussian differential privacy, 2019.

[6] Jinshuo Dong, Aaron Roth, and Weijie Su. Gaussian differential privacy. *Journal of the Royal Statistical Society*, 2021.

[7] Cynthia Dwork and Guy N Rothblum. Concentrated differential privacy. *arXiv preprint arXiv:1603.01887*, 2016.

[8] Cynthia Dwork, Krishnaram Kenthapadi, Frank McSherry, Ilya Mironov, and Moni Naor. Our data, ourselves: Privacy via distributed noise generation. In *Annual International Conference on the Theory and Applications of Cryptographic Techniques*, pages 486–503. Springer, 2006.

[9] Cynthia Dwork, Frank McSherry, Kobbi Nissim, and Adam Smith. Calibrating noise to sensitivity in private data analysis. In *Theory of cryptography conference*, pages 265–284. Springer, 2006.

[10] Cynthia Dwork, Aaron Roth, et al. The algorithmic foundations of differential privacy. *Foundations and Trends® in Theoretical Computer Science*, 9(3–4):211–407, 2014.

[11] Kaiming He, Xiangyu Zhang, Shaoqing Ren, and Jian Sun. Deep residual learning for image recognition, 2015.

[12] Kai Hu. Revisiting Exploding Gradient: A Ghost That Never Leaves. 2022. URL `https://www.andrew.cmu.edu/user/kaihu/Revisiting_Exploding_Gradient.pdf`.

[13] Sergey Ioffe and Christian Szegedy. Batch normalization: Accelerating deep network training by reducing internal covariate shift, 2015.

[14] Alex Krizhevsky. Learning multiple layers of features from tiny images. 2009.

[15] Y. Lecun, L. Bottou, Y. Bengio, and P. Haffner. Gradient-based learning applied to document recognition. *Proceedings of the IEEE*, 86(11):2278–2324, 1998. doi: 10.1109/5.726791.

[16] H. Brendan McMahan, Daniel Ramage, Kunal Talwar, and Li Zhang. Learning differentially private recurrent language models, 2018.

[17] Ilya Mironov. Rényi differential privacy. In *2017 IEEE 30th computer security foundations symposium (CSF)*, pages 263–275. IEEE, 2017.

[18] Opacus. Opacus PyTorch library. Available from opacus.ai.

[19] Herbert Robbins and Sutton Monro. A stochastic approximation method. *The Annals of Mathematical Statistics*, 22(3):400–407, 1951.

[20] Koen Lennart van der Veen, Ruben Seggers, Peter Bloem, and Giorgio Patrini. Three tools for practical differential privacy. *arXiv preprint arXiv:1812.02890*, 2018.

[21] Depeng Xu, Wei Du, and Xintao Wu. Removing disparate impact on model accuracy in differentially private stochastic gradient descent. In *Proceedings of the 27th ACM SIGKDD Conference on Knowledge Discovery and Data Mining*, KDD '21, page 1924–1932, New York, NY, USA, 2021. Association for Computing Machinery. ISBN 9781450383325. doi: 10.1145/3447548.3467268. URL https://doi.org/10.1145/3447548.3467268.

[22] Xinyang Zhang, Shouling Ji, and Ting Wang. Differentially private releasing via deep generative model. *CoRR*, abs/1801.01594, 2018. URL http://arxiv.org/abs/1801.01594.

A   Supplementary Material

As shown in the main paper, the training of resnet-18 for DP-SGD with BC and ALC converges when the added Gaussian noise is small enough. We suspect that this is related to the size of the networks and the complexity of the training dataset. In Section A.1, we work with shallow networks and see if the training of shallow networks on CIFAR10 can converge for larger Gaussian noise. In Section A.2 we train a simple network on the simpler dataset MNIST and investigate whether the Gaussian noise can even be larger. (We remind the reader that the larger the added Gaussian noise, the better the DP guarantee.) In Section A.3, we give evidence that DPSGD with batch clipping preserves the merits of using batch normalization layers in convolutional neural networks. To complete the work, Section A.4 compares ALC with Full Gradient Clipping (FGC) showing that ALC outperforms FGC.

A.1   Lightweight Network on a Complex Dataset: convnet with CIFAR10

We conduct the same experiments as for resnet-18 on the CIFAR10 dataset with a lightweight network (convnet) which consists of 5 layers. The first 4 layers are the combination of a convolutional layer, a batch normalization layer and an average pooling layer followed by CONV-BN-POOLING order. The last layer is a softmax layer. The convent model architecture is defined in Table 1.

Operation Layer	#Filters	Kernel size	Stride	Padding	Output size	Activation function
$Conv2D$	32	3×3	1×1	1×1		ReLu
$BatchnNorm2d$		32×32			$16 \times 16 \times 3$	
$AvgPool2d$		2×2	2×2			
$Conv2D$	64	3×3	1×1	1×1		ReLu
$BatchnNorm2d$		64×64			$8 \times 8 \times 32$	
$AvgPool2d$		2×2	2×2			
$Conv2D$	64	3×3	1×1	1×1		ReLu
$BatchnNorm2d$		64×64			$4 \times 4 \times 64$	
$AvgPool2d$		2×2	2×2			
$Conv2D$	128	3×3	1×1	1×1		ReLu
$BatchnNorm2d$		128×128			$1 \times 1 \times 128$	
$AdaptiveAvgPool2d$		1×1	1×1			
$FC2$	$-$	$-$	$-$	$-$	10	$softmax$

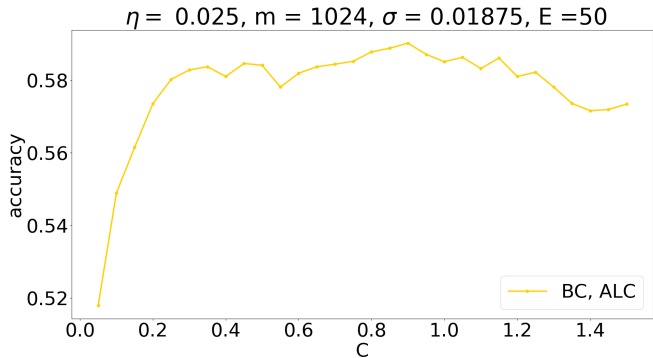Table 1: convnet model architecture with batch normalization layers

Figure 6: Test accuracy of DP-SGD with BC and ALC for convnet with CIFAR10 with respect to various master clipping values C and fixed $\sigma = 0.01875$.

In our first experiment we choose the noise multiplier $\sigma = 0.01875$, batch size $m = 1024$, diminishing learning rate $\eta = 0.025$ with decay value $\eta_{decay} = 0.9$. We vary the master clipping value C as shown in Figure 6. For $C = 0.9$, we achieve 59.02% test accuracy after 50 epochs, which is less than the 67% test accuracy achieved by the resnet-18 model. We observe that the test accuracy increases significantly for $0 < C \leq 0.2$, is stable with some fluctuations for $0.2 < C < 0.9$, and decreases slightly for $C > 0.9$. We conclude that, for noise multiplier $\sigma = 0.01875$, there is a range of C where we see stable performance in terms of test accuracy.

In our second experiment we want to push the lightweight convnet model to the limit where we choose a relatively large $\sigma = 0.5$ with all other hyper-parameters remaining the same. As shown in figure 7, we only achieve 40.58% test accuracy for $C = 0.1$ and we observe that the test accuracy decreases for $C > 0.1$.
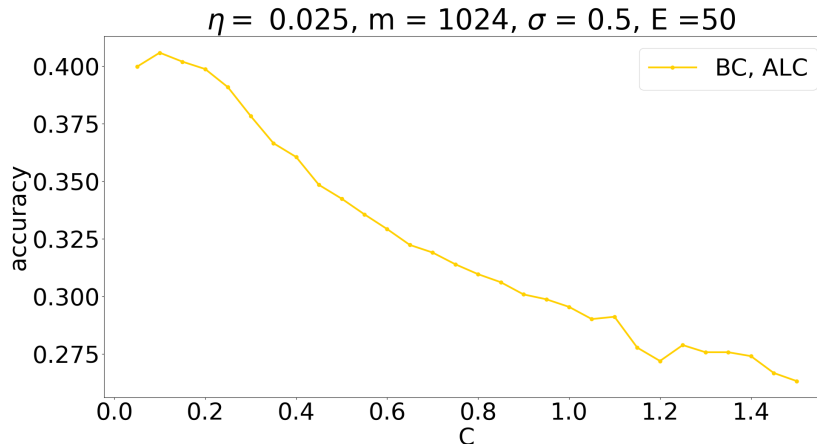
Figure 7: Test accuracy of DP-SGD with BC and ALC for convnet with CIFAR10 with respect to various master clipping values C, fixed $\sigma = 0.5$ and $m = 1024$
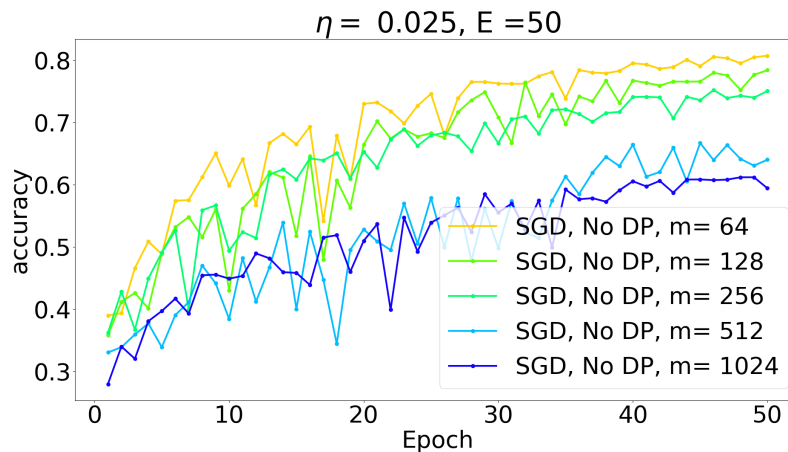

Figure 8: Test accuracies of mini-batch SGD without DP for different mini-batch sizes $m = (64, 128, 256, 512, 1024)$

See Figure 8, our third experiment studies mini-batch SGD without DP for convnet with CIFAR10 as our benchmark. We see that smaller batch sizes yield better accuracy. Specifically, we achieve 80.55% test accuracy for batch size $m = 64$ and 61.19% for batch size $m = 1024$.

This leads us to the fourth experiment, where, by choosing a smaller batch size, we try to increase the test accuracy of DP-SGD with BC and ALC for convnet and CIFAR10 with $\sigma = 0.5$. For example, in Fig 9.a we choose $m = 64$ and vary the master clipping constant C to find the value which gives best test accuracy: We achieve 43.42% test accuracy for $C = 0.14$. Moreover, we also vary the noise multiplier value σ with fixed master clipping value $C = 0.14$ to see whether our model can sustain larger noise. The Figure 9.a shows that the testing accuracy drops $\approx 15\%$ when we increase σ from 0.01 to 0.2 and decreases $\approx 10\%$ more from $\sigma = 0.2$ to $\sigma = 0.6$. Therefore, we choose $\sigma = 0.5$ for the next experiments, where we can achieve $\approx 35\%$ testing accuracy and have better DP guarantee than our resnet-18 experiment.

Our final experiment uses DP-SGD with BC and ALC to train convnet with CIFAR10 for different batch sizes $m = (64, 128, 256, 512, 1024)$; We use master clipping constant $C = 0.14$, initial learning rate $\eta = 0.025$ with decay rate $\eta_{decay} = 0.9$, noise multiplier $\sigma = 0.5$, and number of epochs $E = 50$. We compare with mini-batch SGD without DP with $m = 64$ in Figure 10. Although the accuracy is hurt badly by the Gaussian noise, the lightweight convnet model is still able to converge to $\approx 40\%$ test accuracy while the test accuracy for resnet-18 starts to fall below 40% for $\sigma \geq 0.2$ and only achieves $\approx 20\%$ test accuracy for $\sigma = 0.5$.
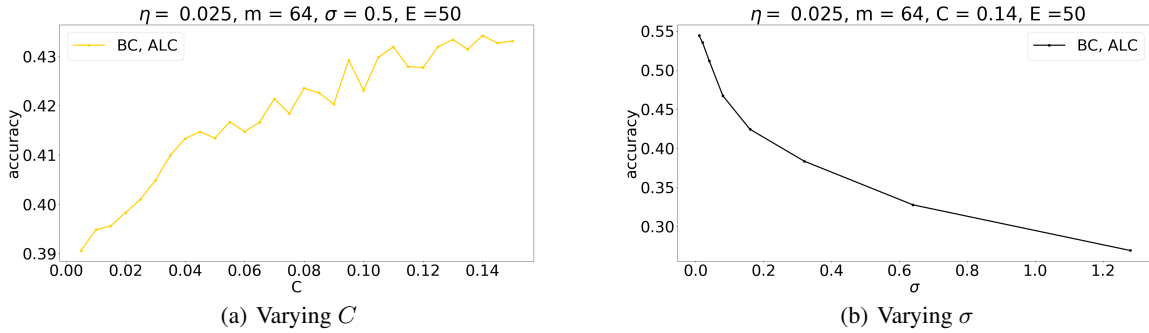
(a) Varying C (b) Varying σ

Figure 9: Test accuracy of DP-SGD with BC and ALC for convnet with CIFAR10 with respect to various master clipping values C and noise multiplier σ with batch size $m = 64$
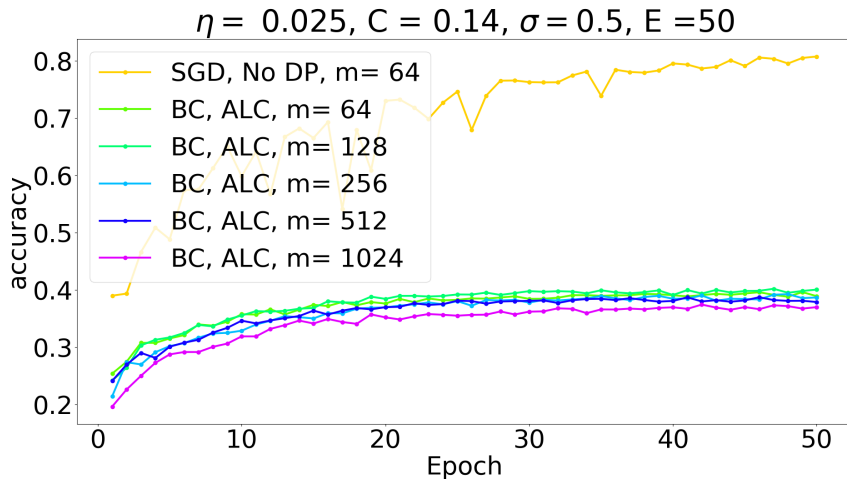

Figure 10: Test accuracies of DPSGD+BC+ALC vs mini-batch SGD without DP for different mini-batch sizes $m = (64, 128, 256, 512, 1024)$

Our experiments show that the deep resnet-18 network is more sensitive to the added Gaussian noise than the lightweight convnet network. This observation opens a new research direction where we want to simplify the neural network model as much as possible for a given dataset type (and corresponding learning task) while maintaining test accuracy and allowing a large enough σ for a reasonable DP guarantee. We expect (given our experiments) to be able to train simpler network models with a larger noise multiplier σ and this yields better privacy. The network simplification should not be too much in that the test accuracy of a trained model with DP noise should still be "good enough."

A.2 Lightweight Network on a Simple Dataset: BN-LeNet-5 with MNIST

We investigate how well our method performs on a simpler dataset compared to CIFAR-10. For this reason we conduct the same experiments of Section A.1 on the MNIST dataset.

MNIST consists of 60,000 training examples and 10,000 testing examples of handwritten digits [15]. Each example is a 28x28 gray-level image. For training, we use the modified version of LeNet-5 [15], where we add a batch normalization layer after each convolutional layer. The details of the modified LeNet-5 architecture (BN-LeNet-5) are described in Table 2. For each training image, we crop a 32×32 region from it with padding of 4, apply a random horizontal flip to the image, and then normalize it with

$$(mean, std) = (0.1307, 0.3081).$$

As before, we fix the noise multiplier $\sigma = 0.5$ and search for a good master clipping constant C. We use DP-SGD with BC and ALC to train the BN-LeNet-5 model with batch size $m = 64$, diminishing step size $\eta = 0.025$ with decaying value $\eta_{decay} = 0.9$ in 50 epochs. See Figure 11, we achieve the best test accuracy 84.80% for $C = 0.2$.

Operation Layer	#Filters	Kernel size	Stride	Padding	Output size	Activation function
$Conv2D$	6	5×5	1×1	0	$28 \times 28 \times 6$	$tanh$
$BatchnNorm2d$		6×6				
$AvgPool2d$		2×2	2×2		$14 \times 14 \times 6$	
$Conv2D$	16	5×5	1×1	0	$10 \times 10 \times 16$	$tanh$
$BatchnNorm2d$		16×16				
$AvgPool2d$		2×2	2×2		$10 \times 10 \times 16$	
$Conv2D$	120	5×5	1×1	0	$5 \times 5 \times 120$	$tanh$
$BatchnNorm2d$		120×120				
$FC1$	–	–	–	–	84	$tanh$
$FC2$	–	–	–	–	10	$softmax$

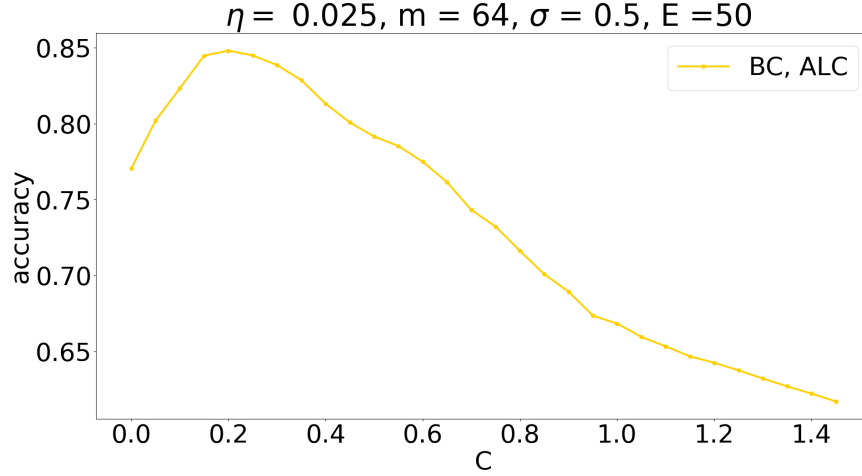Table 2: BN-LeNet-5 model architecture

Figure 11: Test accuracy of DP-SGD with BC and ALC for BN-LeNet-5 with MNIST with respect to various master clipping values C, fixed $\sigma = 0.5$ and $m = 64$

Given $C = 0.2$, we push the BN-LeNet-5 model to the limit by choosing a relatively large noise multiplier σ for which the test accuracy does not drop below 50%. This allows us to see the effect of having a simpler dataset by comparing to the experiments in Section A.1. We achieve 50.38% test accuracy for $\sigma = 2.5$ as shown in Figure 12.b.
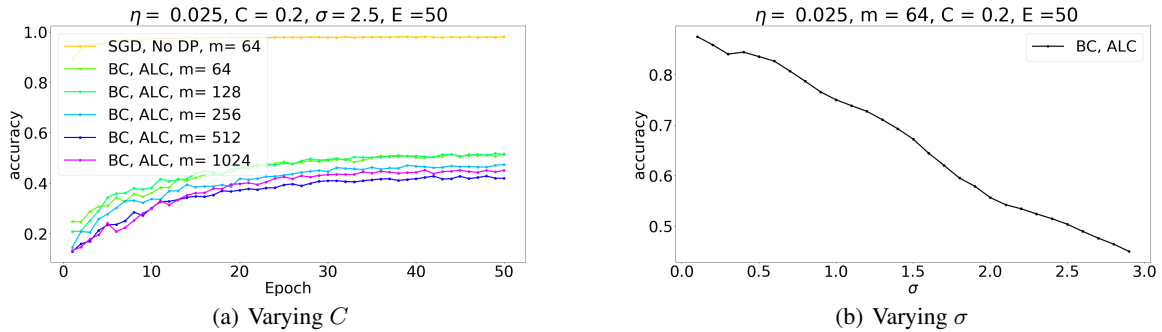

(a) Varying C

(b) Varying σ

Figure 12: Test accuracy of DP-SGD with BC and ALC for BN-LeNet-5 with MNIST with respect to various noise multiplier values σ and master clipping values $C = 0.2$ with batch size $m = 64$

Let $C = 0.2$ and $\sigma = 2.5$, we train the BN-Lenet-5 model with various batch size $m = (64, 128, 256, 512, 1024)$. As shown in Figure 12.a, the test accuracy decreases from 50.38% to 45.11% when we increase the batch size from $m = 64$ to $m = 1024$.

Our main conclusion is that the BN-LeNet-5 model still converges for the large noise multiplier $\sigma = 2.5$ when training on the MNIST dataset. Therefore, the simpler dataset allows us to use more Gaussian noise for differential privacy and this yields an improved Differential Privacy guarantee.

A.3 Batch clipping and Batch Normalization Layer

The concept of a Batch Normalization Layer (BNL) has been introduced in [13] to improve the training speed and testing accuracy for convolutional neural networks. Figure 13 shows that indeed for normal training with SGD without DP batch normalization layers allow a high test accuracy. In this section we investigate how using BNLs helps attaining a higher test accuracy when using DP-SGD with BC and ALC.

(a) convnet with batch normalization layer
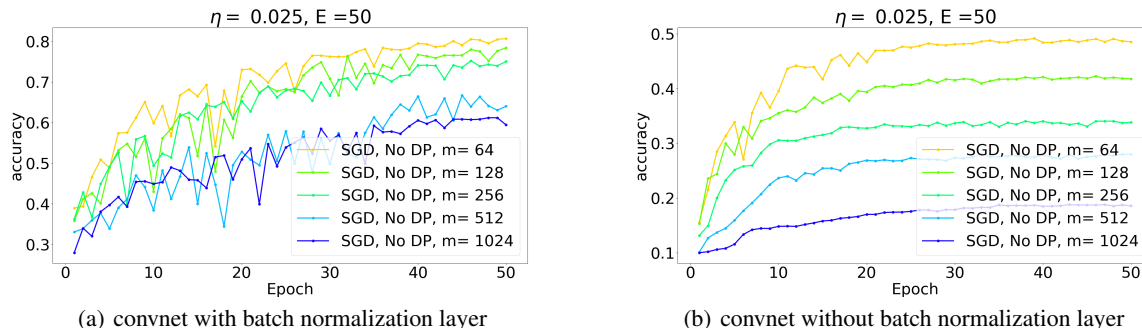
(b) convnet without batch normalization layer

Figure 13: Comparison of the test accuracy of training CIFAR10 with and without BNLs for convnet using SGD without DP.

We compare training convnet 1 with and without BNLs for CIFAR10 by using DP-SGD with BC and ALC. Figure 14 shows that we achieve $\approx 5\%$ higher test accuracy for DP-SGD with batch size $m = 64$, diminishing step size $\eta = 0.025$ with decaying value $\eta_{decay} = 0.9$, master clipping constant $C = 0.14$, noise multiplier $\sigma = 0.5$ and total number of epochs $E = 50$.

(a) convnet with batch normalization layer
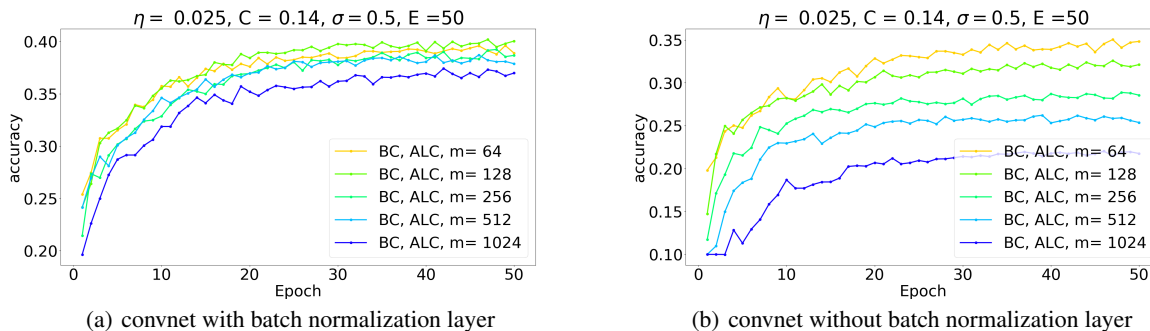
(b) convnet without batch normalization layer

Figure 14: Comparison of the test accuracy of training CIFAR10 with and without BNLs for convnet using DP-SGD with BC and ALC.

We also run experiments with convnet and resnet18 after removing all BNLs for the set-up in Table 3 (as in Section 4 in the main body) where we also consider a diminishing master clipping constant with initial value $C = 0.095$ decaying with rate $C_{decay} = 0.9$ after each epoch.

Figure 15 is for convnet with IC+ALC (as compared to Figure 14 which is for BC+ALC). After removing batch normalization layers in the convnet model, the testing accuracy for IC cannot converge to an acceptable value. After 50 epochs, we only achieve 21.12% test accuracy if we train the model with constant step size and constant master clipping value C for mini-batch size $m = 64$. This shows that batch clipping outperforms individual clipping for convnet without BNLs.

Next, we ask ourselves whether batch clipping still outperforms individual clipping for the more complicated model such resnet18 without BNLs. As shown in Figure 16, we achieve $30\% \sim 40\%$ test accuracy for the various combinations

15

Learning Rate η	0.025
Master Clipping value (C)	0.095
Noise multiplier σ	0.01875
Learning rate decay (η_{decay})	0.9
Clipping value decay (C_{decay})	0.9
Batch size (m)	$[64, 128, 256, 512, 1028]$
Epochs (E)	50

Table 3: Hyperparameter settings

(a) css,constant C

(b) css,diminishing C

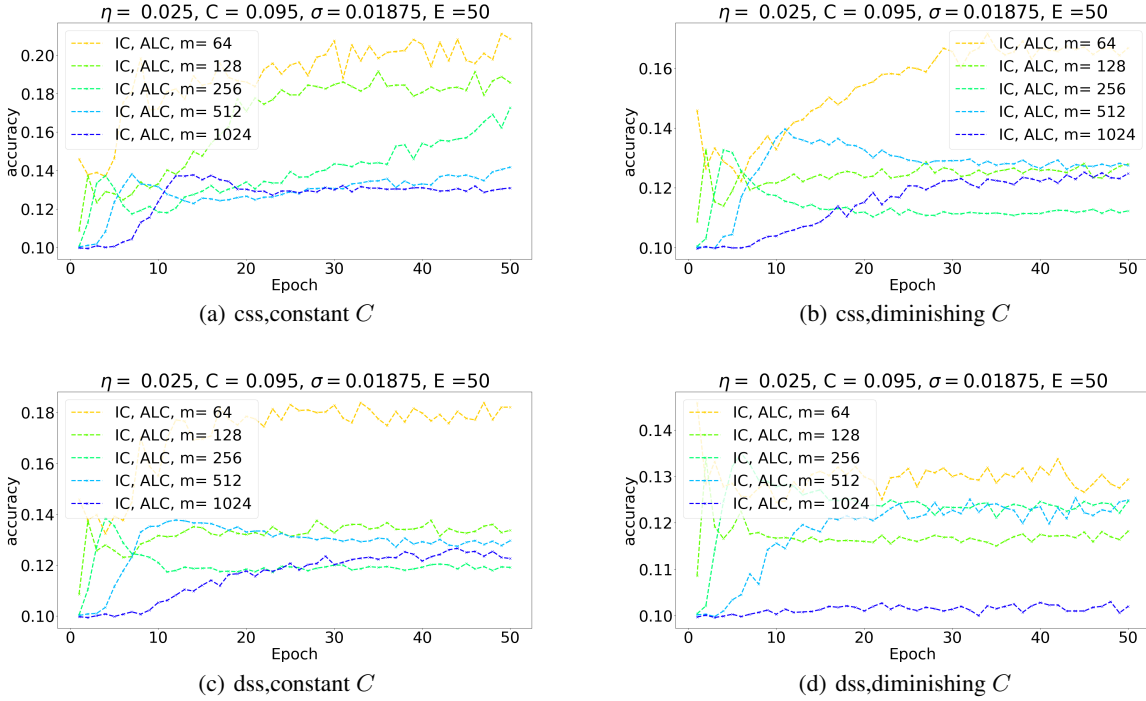(c) dss,constant C

(d) dss,diminishing C

Figure 15: Test accuracy of training CIFAR10 for convnet without BNLs using DP-SGD with IC and ALC. Here, css and dss denote constant step size and diminishing step size, respectively.

of constant and diminishing step size and master constant, respectively (with the best test accuracy close to 40% for constant step size and non-decaying master constant). On the other hand, we only achieve $18\% \sim 22\%$ test accuracy for individual clipping as shown in Figure 17.

A.4 ALC versus FGC

We investigate how ALC compares with Full Gradient Clipping (FGC) under the same Gaussian Noise $N(0, (2C\sigma)^2)$. (FGC means that we clip the full gradient and do not separately clip layers as in ALC.) As shown in Figure 18, we used DP-SGD with BC for 50 epochs in order to train resnet18 with CIFAR10; we use a non-decaying master clipping constant $C = 0.095$, noise multiplier $\sigma = 0.01875$, mini-batch size $m = 64$ and diminishing step size $\eta = 0.025$ with $\eta_{decay} = 0.9$. We achieve 66.66% with ALC and 46.35% with FGC method. This shows evidence that training with ALC leads to better convergence rate as well as better test accuracy.

However, in the above experiment the privacy budget is not the same for ALC versus FGC: See Section 3.2 in ALC we have an extra factor $\sqrt{L}$ in the DP guarantee, where L is the number of layers in the neural network model. Therefore, we also run the same experiment for FGC with discounted noise multiplier $\bar{\sigma} = \sigma/\sqrt{L} = \sigma/\sqrt{62}$ so that both ALC and FGC correspond to the same DP guarantee. The result is shown in Figure 18 and shows that ALC outperforms FGC.
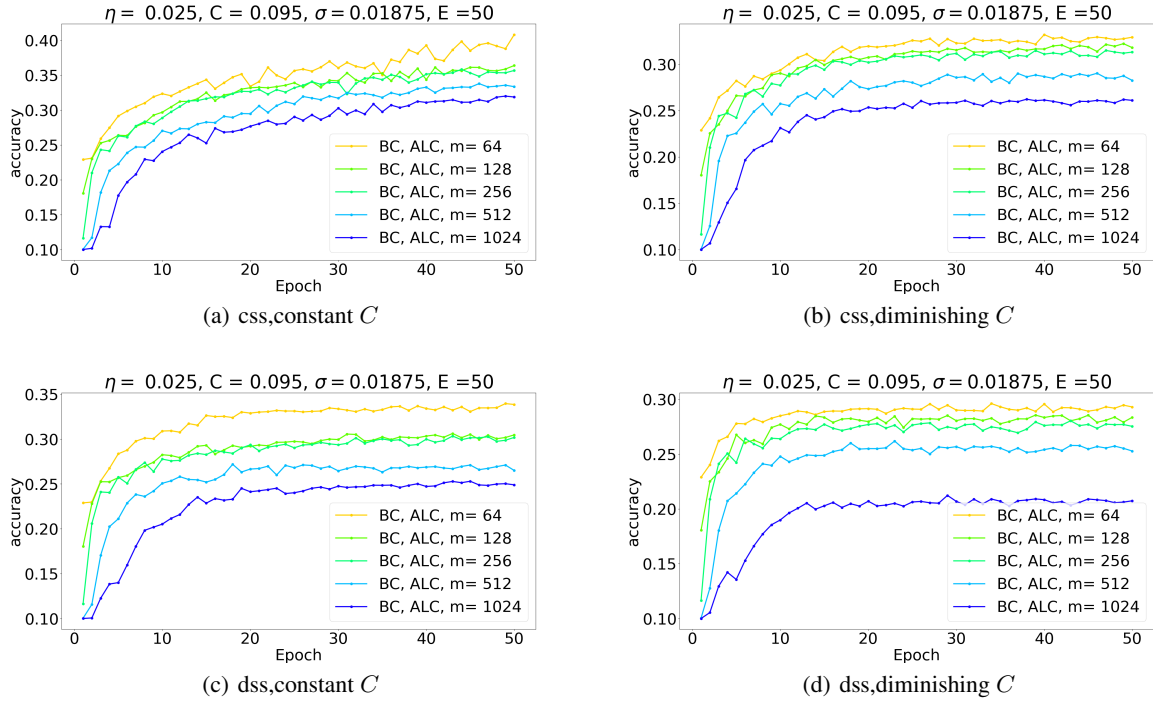
16

Figure 16: Test accuracy of training CIFAR10 for resnet18 without BNLs using DP-SGD with BC and ALC. Here, css and dss denote constant step size and diminishing step size, respectively.
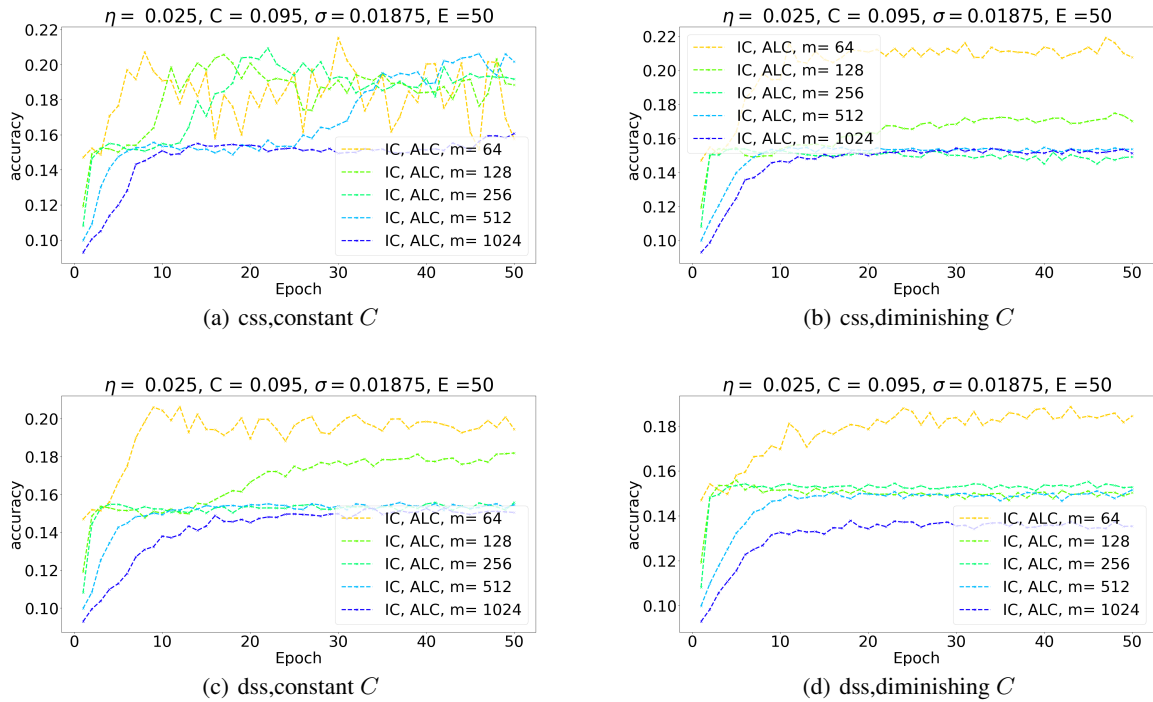

Figure 17: Test accuracy of training CIFAR10 for resnet18 without BNLs using DP-SGD with IC and ALC. Here, css and dss denote constant step size and diminishing step size, respectively.

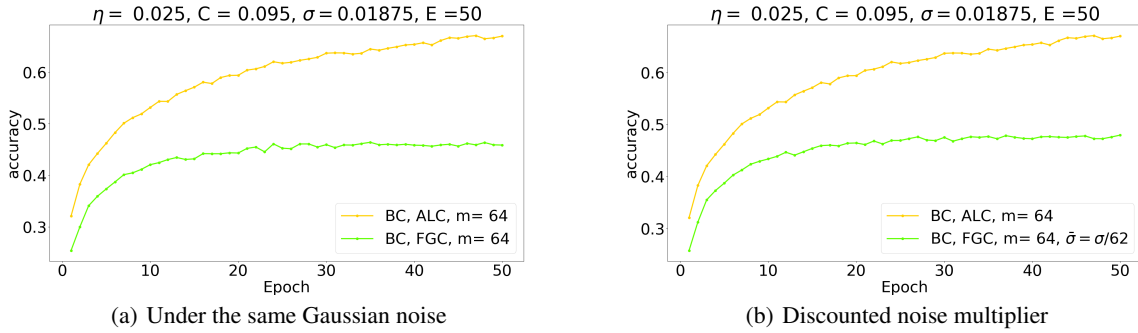(a) Under the same Gaussian noise   (b) Discounted noise multiplier

Figure 18: Test accuracy of DP-SGD of resnet18 with CIFAR10 for BC+ALC versus BC+FGC.

B   Towards Balancing DP Guarantees and Accuracy

In this paper we have discussed how ALC and BC can bring us closer to balancing DP with accuracy. In particular, the focus of this paper is on the ALC and BC techniques for improving robustness against added Gaussian noise for differential privacy. However, we still need additional techniques in order to achieve a practical balance which allows a reasonable accuracy (say at most 10% or 20% drop) together with a DP guarantee which shows a trade-off curve reasonably close to the ideal $1 - \alpha$ curve which represents perfect security.

In Section B.1 we show that ALC+BC as discussed in this paper is not yet sufficient on themselves to find a practical balance: Even though ALC+BC allow us to be significantly more robust against added Gaussian noise for bootstrapping DP, just using these techniques will not yet make training of even lightweight neural network models with less complex training datasets sufficiently robust against the required DP noise for good/solid differential privacy.

One direction of tackling this problem is to enhance and/or optimize the ALC+BC techniques. In Section B.2 we offer suggestions that focus on improving the presented ALC+BC. We leave it to future work to empirically study these possible improvements and optimizations. And we leave it to future work to find altogether new techniques that are complimentary and go beyond ALC+BL.

B.1   Lightweight Neural Network Model with Less Complex Training Dataset

We show that even moving to a lightweight neural network with a less complex training data set still requires additional techniques beyond our BC+ALC and/or improvements of the BC+ALC techniques. We show that BC+ALC as presented in this paper is on its own not yet sufficient even though they make the gap between DP guarantee and accuracy significantly smaller:

We notice that Corollary 5.4 in [6] shows that, for $c >$, if $E = (N/m) \cdot c^2 \to \infty$, then (4) is asymptotically G_μ-DP with $\mu = \sqrt{2} \cdot c \cdot h(\sigma)$ for

$$h(\sigma) = \sqrt{e^{\sigma^{-2}}\Phi(3\sigma^{-1}/2) + 3\Phi(-\sigma^{-1}/2) - 2}.$$

By using their interpretation of their result, we may conclude that (4) is approximately $G_{\sqrt{2} \cdot c \cdot h(\sigma)}$ for $c = \sqrt{Em/N}$ for concrete large N and relatively small E and m. Including ALC means that we need to substitute $\sigma/\sqrt{L}$ for σ.

For $\sigma = 0.01875$, we have $h(\sigma/\sqrt{L}) \approx \sqrt{e^{(\sigma/\sqrt{L})^{-2}}} = e^{L\sigma^{-2}/2}$, i.e., a very very large number leading to no useful DP guarantee even for large datasets (with large N). In other words, σ cannot be too small. Even $\sigma = 0.5$ with $L = 62$ for resnet-18 leads to $h(\sigma/\sqrt{L}) = \sqrt{e^{62 \cdot 4}\Phi(3 \cdot \sqrt{62}) + 3\Phi(-\sqrt{62}) - 2}$ which is prohibitively large for achieving a good DP guarantee. Figure 5 shows that choosing a larger $\sigma > 0.5$ for obtaining a better DP guarantee gives too much noise resulting in a poor test accuracy of at most 20%, which is unacceptable. We conclude that resnet-18 and CIFAR10 represent a too deep neural network and complex dataset for a good balance between test accuracy and DP guarantee when using DP-SGD with our BC and ALC improvements. For now, we see that BC and ALC are two steps toward a better balance (after we are able to achieve convergence where this was not possible before for the original DP-SGD with IC) and that more techniques are needed for deep neural network models with complex training datasets.

Section A.1 shows experiments for the lightweight convnet model with the complex CIFAR10 dataset which achieves a better $\approx 40\%$ test accuracy – this demonstrates that a lightweight neural network model is more robust against noise

and is better suitable for training with DP-SGD with BC and ALC. Section A.2 shows experiments for the lightweight BN-LeNet-5 model with the simple MNIST dataset which, if restricted to 50% accuracy (for proper comparison with the 40% test accuracy for convnet with CIFAR10), allows a much larger $\sigma = 2.5$ resulting in a much improved $G_{0.52}$-DP guarantee ($h(\sigma/\sqrt{L}) = 1.513$ with $L = 8$; $m = 64$, $N = \frac{9}{10} \cdot 60000$, $E = 50$).

A smaller $\sigma = 1.5$ (see Figure 12.b in Section A.2) achieves a better balance of $\approx 67\%$ test accuracy with $\approx G_{1.99}$-DP ($h(\sigma/\sqrt{L}) = 5.783$). For a factor 15 larger dataset we would be able to improve $G_{1.99}$-DP to the better $G_{0.51}$-DP guarantee. We conclude that a more lightweight model and/or less complex (and larger) training dataset can potentially lead to a better balance between test accuracy and DP guarantee using the proposed BC and ALC techniques. Nevertheless, we will even want to improve $G_{0.51}$ to some trade-off function more like $G_{0.01}$ such that hypothesis testing indeed resembles a random guess. To date, this remains an open problem – our ALC+BC techniques provide a step forward, but more complimentary techniques are needed.

B.2 Towards Improving/Optimizing ALC+BC

From an accuracy perspective we see that $\sigma = 1.5$ (as mentioned above) or larger σ may be needed even for a more lightweight network model with a less complex training dataset. For large σ, we notice that a Taylor series expansion of $h(\sigma)$ shows a linear dependency on $1/\sigma$. This shows that μ in a G_μ-DP guarantee for ALC scales with $\sqrt{L}$ (since, as discussed before, ALC requires a factor $\sqrt{L}$ smaller σ if we want to keep the same G_μ-DP guarantee). The linear dependency of μ on $\sqrt{L}$ is due to the fact that there is no subsampling effect for the separate layers within a gradient computation; the leakage is directly composed over all the layers for a single gradient computation (without using a subsampling operator as is done in the general analysis leading to (4)). For this reason, it is advantageous to group layers that have similar clipping constant and clip the group rather than the individual layers within the group. E.g., Figure 1 indicates we may use about 4 groups of layers representing a very small norm, to medium and larger norms. This reduces $L = 62$ down to $L = 4$ for resnet-18. Also, notice that the unexplored sparsification trick mentioned in Section 3.4 may offer another improvement.

Our discussion shows that as future work, we need to further optimize the promising ALC technique. One tempting direction is to not use a single training sample ξ for updating all the layer gradients, but to use ξ for a single layer gradient. So, rather than using a data sample ξ for computing updates for all the layer gradients, we can think of using a data sample ξ for updating just one of the layer gradients. Together with ξ we choose one of the L layers at random. In this way we still train all the layers. We notice that this approach means that we have subsampling for each layer gradient and we do not pay the composition price of $\sqrt{L}$ as explained in 3.2. However, one can think of this as L separate learning tasks, each costing the same amount of training as the original learning task which learn the full weight vector across all layers at once. This means a composition of L leakages and we again pay the price of $\sqrt{L}$ since $G_\mu^{\otimes L} = G_{\sqrt{L} \cdot \mu}$. Or, equivalently, one can argue that we need L times more rounds in order to train the full weight vector, i.e., a factor L more epochs, hence, the $\sqrt{L}$ factor penalty after composing over all the epochs. So, this idea still does not improve the sought-after balance between DP guarantee and accuracy since we now have proper amplification from subsampling but at the price of L times more rounds, and this cancels out, that is, no improvement.

Based on the above discussion we would like to somehow only clip the overall full gradient while still keeping the better robustness against DP noise of ALC which requires layerwise clipping. Suppose that we associate a multiplication factor $m_j \geq 1$ to each layer j. We proceed as follows:

1. As before, we first compute the full gradient composed of layer gradients:

$$\nabla_w f(w; \xi) = (\nabla_{w_1} f(w; \xi) || .... || \nabla_{w_L} f(w; \xi)).$$

2. We use the multiplication factors m_j, $1 \leq j \leq L$, to compute

$$\{\nabla_w f(w; \xi)\}_{m_1, ..., m_L} = (m_1 \cdot \nabla_{w_1} f(w; xi) || .... || m_L \cdot \nabla_{w_L} f(w; \xi)).$$

3. Now we perform full gradient clipping (FGC) with clipping constant C:

$$[\{\nabla_w f(w; \xi)\}_{m_1, ..., m_L}]_C.$$

    We use this in computing formulas (the a_h) leading to the noised update U. Notice again that we can use the IC or BC approach in these formulas.

The differential privacy argument follows the line of thinking of our analysis of BC in Section 3.1. Since we use FGC, we do not pay the $\sqrt{L}$ penalty. This will significantly improve the trade-off function as discussed in Section B.1.

What about robustness against the added Gaussian DP noise? The server receives a noised update of the form

$$U = (U_1||...||U_L).$$

The server divides by the multiplication factors and computes

$$(U_1/m_1||...||U_L/m_L)$$

with which the global model is updated. The effect of the proposed trick using multiplication factors m_j is that dividing by the multiplication factors retrieves the original layer gradients – if there is no clipping noise. In this process we reduce the added Gaussian noise, since the noises are divided by the factor $m_j \geq 1$. In our ALC we estimate the expected norm of each layer j denoted by e_j. We equate M to the maximum of all e_j. We compute layer clipping constants $C \cdot e_j/M$. In the above approach based on multiplication factors we may define $m_j = M/e_j$. Since this will increase each layer norm to M in expectation, we will want to choose a higher overall clipping constant C in FGC (as compared[¶] to the master clipping constant C used in ALC). We see that the proposed new trick on one hand remains robust to Gaussian noise added to layers that have a small norm compared to other layers. On the other hand C needs to be fine-tuned and may be larger than the C of ALC, which means that the overall added noise is larger and makes this solution less robust. Concluding, we have the original DP guarantee without $\sqrt{L}$ penalty, while we make sure that layer gradients with small norms get multiplied by a large m_j so that the effect of the added noise for that layer is not going to be overpowering. This is also the goal which ALC wants to achieve. We leave it to future work to experiment with multiplication factors and in this sense optimize over ALC and/or find a better balance between DP guarantee and test accuracy.

As a final remark, we notice that we do not need to restrict ourselves to using BC, we may use GBC which allows momentum based update rules. We leave it to future work to find out whether this can lead to more robustness against added Gaussian DP noise.

[¶]We can use the same collecting-layers-into-4-groups argument for resnet18 with which we started this section and conclude that the clipping constant corresponding to the use of multiplication factors is about $\sqrt{4} = 2$ larger.